

Document downloaded from:

<http://hdl.handle.net/10251/81753>

This paper must be cited as:

Rutkowska, M.; Macina, D.; Piwowarska, Z.; Gajewska, M.; Díaz Morales, UM.; Chmielarz, L. (2016). Hierarchically structured ZSM-5 obtained by optimized mesotemplate-free method as active catalyst for methanol to DME conversion. *Catalysis Science and Technology*. 6(13):4849-4862. doi:10.1039/c6cy00040a.



The final publication is available at

<http://dx.doi.org/10.1039/c6cy00040a>

Copyright Royal Society of Chemistry

Additional Information

## Hierarchically structured ZSM-5 obtained by optimized mesotemplate-free method as active catalyst for methanol to DME conversion

Received 00th January 20xx,  
Accepted 00th January 20xx

DOI: 10.1039/x0xx00000x

[www.rsc.org/](http://www.rsc.org/)

M. Rutkowska<sup>1\*</sup>, D. Macina<sup>1</sup>, Z. Piwowarska<sup>1</sup>, M. Gajewska<sup>2</sup>, U. Díaz<sup>3</sup>, L. Chmielarz<sup>1</sup>

In the presented studies, a new synthesis method of hierarchical porous materials with ZSM-5 zeolite properties was applied. The proposed method is based on the acidification of the zeolite seeds slurry using HCl solution, followed by hydrothermal treatment enabling the aggregation of zeolite nanoseeds with the formation of the interparticle mesoporous structure. An influence of duration of zeolite parent mixture aging before and after acidification on the resulting properties of the samples was investigated. The physicochemical properties of the obtained micro-mesoporous samples were analyzed using techniques such as: N<sub>2</sub>-sorption measurements, X-ray diffraction, TG analysis, NH<sub>3</sub>-TPD and electron microscopy. In a second part of the studies an influence of the modified zeolite sample parameters (such as porosity, acidity and crystallinity) on their catalytic activity for dimethyl ether (DME) synthesis from methanol was studied. DME is considered as a future clean diesel fuel alternative and a develop in its synthesis methods is currently under high scientist interest. It was shown that modification of the porous structure and acidity of the zeolitic samples strongly influences their catalytic activity, selectivity and stability for process of DME synthesis. The micro-mesoporous samples, despite significantly lower acidity, exhibited high catalytic activity (similar to conventional ZSM-5 zeolite) and enhanced selectivity to DME as well as high stability in a long term catalytic test (higher resistance for the formation of coke deposits) in comparison to standard MFI-type zeolites.

### 1. Introduction

Hierarchical zeolites, containing both micro- and mesopores are a new and rapidly developing group of materials. Among this group, special scientist's interest was devoted to generation of mesopores in the ZSM-5 zeolite structure (MFI topology), which is known to be very active in many catalytic reactions. It is expected that the presence of mesopores should minimize internal diffusion limitations and enhance the overall effectiveness of the catalytic processes. During recent years different approaches were applied to synthesize micro-mesoporous ZSM-5 zeolite. One of the most widely studied methods were based on destructive post-synthesis treatments - desilication and dealumination (controlled removal of framework Si and Al in basic and acidic medium, respectively) [1-4]. Moreover, many constructive methods were proposed in the literature, such as carbon, polymer or soft (surfactant) templating [5-7] or methods based on the synthesis and controlled alignment of ZSM-5 sheets. The group of prof. Ryoo [8, 9] synthesized MFI nanosheets of 2 nm thickness using an organic surfactant

functionalized with a diquatery ammonium group in the head (e.g. C<sub>22</sub>H<sub>45</sub>-N<sup>+</sup>(CH<sub>3</sub>)<sub>2</sub>-C<sub>6</sub>H<sub>12</sub>-N<sup>+</sup>(CH<sub>3</sub>)<sub>2</sub>-C<sub>6</sub>H<sub>13</sub>) as a structure directing agent for intercalation of silica pillars into the zeolite interlayer space. The diameter of mesopores generated in the interlayer space could be tailored by the modification of the surfactant structure, especially hydrocarbon tail length. Zhang et al. [10] reported successful synthesis of self-pillared nanosheets of MFI (using one-step hydrothermal synthesis method) with the house-of-cards structure and mesopores in the range of 2-7 nm.

From the economic and environmental point of view the most promising seems to be the one-pot synthesis methods, resulting in obtaining of hierarchical materials in a one-step procedure without the use of expensive surfactants for the mesopores formation. One of the possible options is a mesotemplate-free method, basing on the controlled aggregation of zeolite nanoseeds [11] with the formation of the interparticle mesoporous structure. This approach was previously applied by Rutkowska et al. [12, 13] and Van Oers et al. [14, 15] and concerned the synthesis of micro-mesoporous materials with Beta zeolite properties. In this work authors presented a new method of micro-mesoporous ZSM-5 synthesis using mesotemplate-free method and the catalytic efficiency of the obtained materials in the synthesis of dimethyl ether (DME) from methanol.

Dimethyl ether, due to its unique properties such as high cetane number, lack of C-C bond, vapor pressure similar to LPG and atoxicity, gained a great scientist attention as a promising clean

<sup>1</sup>Jagiellonian University, Faculty of Chemistry, Ingardena 3, 30-060 Kraków, Poland

<sup>2</sup>AGH University of Science and Technology, Academic Centre for Materials and Nanotechnology, Mickiewicza 30, 30-059 Kraków, Poland

<sup>3</sup>Instituto de Tecnología Química, UPV-CSIC, Universidad Politécnica de Valencia, Avenida de los Naranjos, s/n, 46022 Valencia, Spain

\*Corresponding author. Tel.: +48 126632096, fax: +48 126340515. E-mail address: rutkowsm@chemia.uj.edu.pl (M. Rutkowska)

alternative fuel [16, 17]. DME can be used as an LPG (similar physico-chemical properties allow the use of existing infrastructures for transportation and storage) and diesel fuel substitute (lower soot emission in comparison to conventional fuels). Moreover, DME can be used as a petroleum gas for heating and home cooking (burning with visible blue flame) or as a substrate of many chemical reactions (low-poisoning alternative of methanol) e.g. being converted to light olefins or aromatics. DME can be synthesized directly from syngas (produced from natural gas, coal or biomass) using bifunctional catalyst ( $2\text{CO} + 4\text{H}_2 \rightarrow \text{CH}_3\text{OCH}_3 + \text{H}_2\text{O}$ ) or by indirect method from methanol using acid catalyst ( $2\text{CH}_3\text{OH} \rightarrow \text{CH}_3\text{OCH}_3 + \text{H}_2\text{O}$ ). Concluding, a growing awareness of climate change, air pollution and continuously increasing energy consumption make DME an attractive green alternative to cut down the greenhouse gases emission and to recycle the stored resources of  $\text{CO}_2$  (in case of direct synthesis method).

ZSM-5 zeolite was found to be active and stable catalyst of MTD process (methanol to DME), especially in the presence of water. The high catalytic activity of this zeolite results from the presence of Brønsted acid sites, responsible for adsorption and conversion of methanol [18]. The strength of acid sites is very important in MTD process because too strong acid sites may result in carbonaceous species deposition, which hinder the access of methanol to active centers and block the pores of zeolite. This undesired effect can be overcome by the modification of the porous structure and acidity of ZSM-5 zeolite [19, 20].

To the best of our knowledge only a few of papers regarding the catalytic performance of micro-mesoporous systems with ZSM-5 zeolite properties in the synthesis of DME were published. In our previous studies [21] we examined micro-mesoporous ZSM-5 obtained by desilication of parent zeolite with 0.1 M solution of NaOH for 1, 2 and 4 h. Desilicated samples exhibited higher catalytic activity and stability in DME synthesis in comparison to conventional zeolite. Wei et al. [22] investigated catalytic activity of desilicated ZSM-5 (using 0.2 M NaOH) with different Si/Al ratio and reported an improvement of selectivity to DME. This effect was related to the enhanced diffusion capability in the micro-mesoporous samples. Yang et al. [23] examined hierarchical ZSM-5 synthesized using simultaneously two kinds of templates for micro- and mesopores generation (tetrapropylammonium hydroxide and dimethyldiallyl ammonium chloride acrylamide copolymer, respectively). Mesoporous ZSM-5 obtained by this method exhibited better stability (higher resistance for coke formation) in comparison to conventional ZSM-5. Another interesting group of micro-mesoporous catalysts for MTD reaction are ZSM-5/MCM-41 composites (showing better selectivity to DME in comparison to conventional ZSM-5), prepared by hydrothermal technique using nanosized ZSM-5 particles [24-26].

Taking into account the benefits resulting from the presence of mesopores in the structure of the catalyst with MFI topology in MTD reaction, a new one-step method of hierarchical ZSM-5 synthesis was proposed. In this work an influence of the hydrothermal synthesis parameters on the physicochemical properties of the micro-mesoporous samples and their activity, selectivity and stability for dimethyl ether synthesis from methanol was studied.

## 2. Experimental methods

### 2.1. Catalysts preparation

The samples with ZSM-5 zeolite properties were prepared according to the modified procedure described in 'Verified Synthesis of Zeolitic Materials' for high alumina ZSM-5 [27]. Tetrapropylammonium hydroxide (TPAOH, 20% in  $\text{H}_2\text{O}$ , Sigma-Aldrich) was used as a structure-directing agent, while tetraethyl orthosilicate (TEOS, 98%, Sigma-Aldrich) and  $\text{NaAlO}_2$  (Sigma-Aldrich) as silica and aluminium sources, respectively.

In a first stage seeding gel was prepared by mixing of TPAOH with an aqueous solution of NaOH, followed by a dropwise addition of TEOS. The resulting slurry was mixed for 1 h and then hydrothermally aged in autoclaves at  $100^\circ\text{C}$  for 16 h.

In a second step the synthesis gel was prepared by mixing of 5 g of the obtained earlier seeding gel with a water solution of NaOH and  $\text{NaAlO}_2$ , followed by a dropwise addition of TEOS. The resulting solution with the molar composition:  $\text{SiO}_2 : 0.03 \text{ Al}_2\text{O}_3 : 0.11 \text{ Na}_2\text{O} : 30 \text{ H}_2\text{O}$  (exclusive of seeding gel) was hydrothermally treated at  $150^\circ\text{C}$  for 7 days (in case of conventional ZSM-5) and for 24, 48 or 72 h (in case of the hierarchical porous samples). After appropriate time (24, 48 or 72 h) of hydrothermal aging the protozeolitic seeds were acidified in a proportion of 5 mL of concentrated HCl per 10 mL of the nanoseeds slurry. Subsequently, the acidified slurries were hydrothermally treated for the second time at  $150^\circ\text{C}$  for 144, 120 or 96 h, yielding micro-mesoporous ZSM-5 zeolite. After aging periods all the autoclaves were quenched and the samples were filtered, washed with distilled water, dried in ambient conditions and calcined at  $600^\circ\text{C}$  for 6 h.

The as-synthesized samples were denoted as follows: as-ZSM-5 (aging duration before acidification -24, 48 or 72 h/ aging duration after acidification -144, 120 or 96 h). The aging duration after acidification was adjust to keep the total aging duration of 7 days (as in case of conventional ZSM-5). Among this group of the samples an optimum aging duration before acidification of 48 h was chosen. For this sample an influence of the aging duration after acidification on its physico-chemical properties was determined. This series of the samples was denoted as as-ZSM-5 (48/ aging duration after acidification - 24 or 48). All the sample codes and the parameters of their synthesis are presented in Tab.1.

**Table 1** Sample codes and synthesis conditions

Sample code	Aging duration before acidification /h	Aging duration after acidification /h	Total aging duration /days
as-ZSM-5	---	---	7
as-ZSM-5 (24/144)	24	144	7
as-ZSM-5 (48/120)	48	120	7
as-ZSM-5 (72/96)	72	96	7
as-ZSM-5 (48/24)	48	24	3
as-ZSM-5 (48/72)	48	72	5

The as-synthesized samples (in Na-forms in case of the hierarchical samples partially H-exchanged during acidification) were triple

exchanged with a 0.5 M solution of  $\text{NH}_4\text{NO}_3$  (Sigma-Aldrich) at 80°C for 1 h, filtered, washed with distilled  $\text{H}_2\text{O}$  and dried in ambient conditions. Finally, the samples were calcined at 600°C for 6 h to convert them to H-forms.

## 2.2. Catalysts characterization

Textural properties of the samples were determined by  $\text{N}_2$  sorption at -196°C using a 3Flex v1.00 (Micromeritics) automated gas adsorption system. Prior to the analysis, the samples were degassed under vacuum at 350°C for 24 h. The specific surface area ( $S_{\text{BET}}$ ) of the samples was determined using BET (Braunauer-Emmett-Teller) model according to Rouquerol et al. recommendations [28]. The micropore volume and specific surface area of micropores were calculated using the Harkins and Jura model (t-plot analysis, thickness range 0.55-0.85 nm). Mesopore volume was calculated from desorption branch using BJH model (Kruk-Jaroniec-Sayari empirical procedure) in the range of 17-300 Å.

The X-ray diffraction (XRD) patterns of the samples were recorded using a Bruker D2 Phaser diffractometer. The measurements were performed in the 2 theta range of 5 - 50° with a step of 0.02°.

Thermogravimetric measurements were performed using a TGA/SDTA851e Mettler Toledo instrument connected with quadrupole mass spectrometer ThermoStar (Balzers). The samples were heated in a flow of synthetic air (80 mL/min) with the ramping of 10°C/min, in the temperature range of 70-1000°C.

The Si/Al ratio in the samples was analyzed by means of atomic absorption spectroscopy (Spectra AA 10 Plus, Varian).

Surface acidity (concentration and strength of acid sites) of the samples was studied by temperature-programmed desorption of ammonia ( $\text{NH}_3$ -TPD). The measurements were performed in a flow microreactor system equipped with QMS detector (UMS TD Prevac). Prior to ammonia sorption, a sample was outgassed in a flow of pure helium at 600°C for 30 min. Subsequently, microreactor was cooled to 70°C and the sample was saturated in a flow of gas mixture containing 1 vol.% of  $\text{NH}_3$  diluted in helium for about 120 min. Then, the catalyst was purged in a helium flow until a constant base line level was attained. Desorption was carried out with a linear heating rate (10°C/min) in a flow of He (20 ml/min). Calibration of QMS with commercial mixtures allowed recalculating detector signal into the rate of  $\text{NH}_3$  evolution.

Transmission electron microscopy (TEM) investigations were carried out using a FEI Tecnai TF20 X-TWIN (FEG) microscope, equipped with EDAX energy dispersive X-ray (EDX) detector, at an accelerating voltage of 200 kV.

The chemical nature of the coke deposit formed during catalytic reaction was studied by UV-vis-DR spectroscopy. The measurements were performed using an Evolution 600 (Thermo) spectrophotometer in the range of 200-900 nm with a resolution of 2 nm.

## 2.3. Catalytic tests

Catalytic experiments for the process of DME synthesis from methanol were performed in a fixed-bed quartz microreactor

system under atmospheric pressure in the temperature range from 100 to 325°C in intervals of 25°C. For each test, 0.1 g of catalyst with a particle size between 0.160 and 0.315 mm was outgassed in a flow of pure helium at 300°C for 1 h. After cooling down to 100°C the gas mixture containing 4 vol.% of methanol diluted in pure helium (total flow rate of 20 ml/min) was supplied into microreactor using an isothermal saturator (0°C). To avoid any product condensation during the reaction run, the gas lines were heated to 120°C using heating tapes. The outlet gases were analyzed using a gas chromatograph (SRI 8610C) equipped with Haysep D column, methanizer and FID detector. Additionally, the catalytic stability tests (50 h of continuous work) at 250°C were carried out for the H-ZSM-5 and H-ZSM-5 (48/120) samples.

## 3. Results and discussion

### 3.1. Synthesis and characterization

Textural parameters of the as-synthesized samples, determined by nitrogen sorption measurements, are presented in Tab. 2. The BET surface area of the hierarchical samples is lower in comparison to reference conventional as-ZSM-5. The value of  $S_{\text{BET}}$  increased with increasing of the aging duration before acidification to reach 300  $\text{m}^2/\text{g}$  after 48 h (it seems that further prolongation of aging duration before acidification does not significantly influence value of  $S_{\text{BET}}$ ). These changes were accompanied by a decrease in micropore volume and area of the acidified samples in comparison to conventional zeolite. Also in case of these parameters we observed an increase with increasing of the aging duration before acidification to obtain a constant level after 48 h. However, a decrease in microporosity volume observed after acidification occurred in favor of a significant increase (four times in case of as-ZSM-5 (48)) in mesopore volume of the hierarchical samples. An increase in volume of mesopores proves the successful generation of mesopores in the acidified as-ZSM-5 (48/120) and as-ZSM-5 (72/96) samples.

**Table 2** Textural properties of the as-synthesized samples determined from the  $\text{N}_2$ -sorption measurements and Si/Al ratio of the samples

Sample code	$S_{\text{BET}}$ / $\text{m}^2/\text{g}$	$S_{\text{MIC}}$ / $\text{m}^2/\text{g}$	$V_{\text{MIC}}$ / $\text{cm}^3/\text{g}$	$V_{\text{MES}}$ / $\text{cm}^3/\text{g}$	Si/Al
as-ZSM-5	379	371	0.145	0.024	12
as-ZSM-5 (24/144)	30	20	0.009	0.019	18
as-ZSM-5 (48/120)	300	277	0.119	0.105	22
as-ZSM-5 (72/96)	301	279	0.118	0.077	19
as-ZSM-5 (48/24)	157	114	0.049	0.069	34
as-ZSM-5 (48/72)	195	165	0.071	0.092	35

Basing on the textural parameters obtained by  $\text{N}_2$ -sorption measurements it could be concluded that the duration of nucleation of zeolitic seeds before acidification is a very important parameter affecting the final properties of the hierarchical samples. In case of ZSM-5 zeolite conducting of the hydrothermal ageing process for 24 h was not enough to generate the microporous

structure, however the extending of aging duration to 48 h seems to be enough to crystallize MFI protozeolitic seeds (giving about 80% of as-ZSM-5 micropore volume) and the prolongation of this time does not significantly influence the microporosity development of the samples. On the other side the acidification of the synthesis gel resulted in generation of significant mesoporosity, in case of both the samples as-ZSM-5 (48/120) and as-ZSM-5 (72/96), greater than in case of as-ZSM-5 and as-ZSM-5 (24/144). Taking into account the economic issues (shorter aging duration at 150°C) the 48 h aging procedure was chosen as the optimal and in the next step of our research an influence of the aging duration after acidification on the textural parameters of the samples was verified.

The shortening of the aging duration after acidification resulted in a decrease of all textural parameters, both related to micro- and mesoporosity of the samples. Thus, it could be concluded that the crystallization time after acidification also plays a very important role in the formation of the hierarchical porous structure.

The nitrogen adsorption-desorption isotherms recorded for the as-synthesized samples are shown in Fig. 1. The isotherm of type I(a) (according to the IUPAC classification [29]), characteristic of microporous structure, was obtained for the as-ZSM-5 sample (Fig. 1a). While, in case of the acidified samples the adsorption-desorption isotherms of IV(a) type with hysteresis loops characteristic of mesoporous materials were obtained.

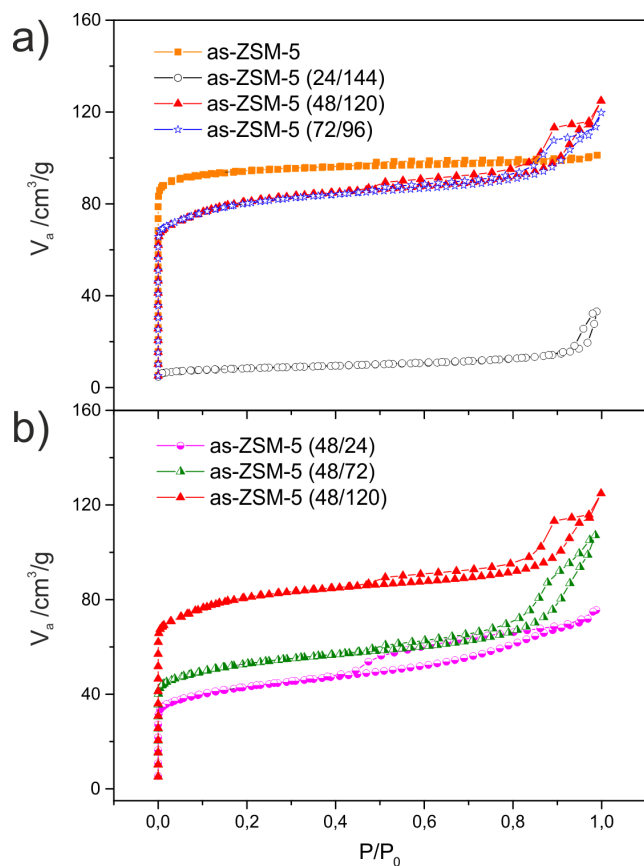


**Fig. 1** Nitrogen adsorption-desorption isotherms of the as-synthesized samples aged for different times before (a) and after (b) acidification

The very low value of adsorbed N<sub>2</sub> volume in case of the as-ZSM-5 (24/144) sample, connected with a lack of an uptake step at very low  $p/p_0$  proved that 24 h of hydrothermal aging before acidification was not enough to effectively create the microporous ZSM-5 structure. In case of as-ZSM-5 (48/120) and as-ZSM-5(72/96) the shape of hysteresis loop can be classified as H5 type (associated with the pore structures containing both open and partially blocked mesopores). A very interesting change in the shape of the hysteresis loop was observed after modification of the aging duration after acidification (Fig. 1b).

Together with the shortening of the aging time after acidification the loop of type H5 changed for the loop of H4 type (often obtained in case of mesoporous zeolites). Thus, it could be concluded that the duration of hydrothermal treatment after acidification strongly influences the shape of created mesopores.

The XRD powder patterns of the as-synthesized samples are shown in Fig. 2. A diffractogram of as-ZSM-5 (Fig. 2a) contains all reflections characteristic of the MFI topology [27], what proves the successful synthesis of parent zeolite. The synthesis modification through the acidification resulted in a decrease of the reflections intensity. In case of as-ZSM-5 (48/120) and as-ZSM-5 (72/96) the structure of MFI topology was preserved, however, in case of as-ZSM-5 (24/144) a broad reflection at about  $15-30^\circ 2\theta$ , assigned to amorphous silica [12] was found. For this sample only low-intensive reflections characteristic of the ZSM-5 structure were identified. These results are in agreement with the N<sub>2</sub> sorption studies and prove that 24 h of zeolite parent mixture crystallization before acidification was not enough to create the MFI structure, instead of which the amorphous material was formed. Fig. 2b shows the diffractograms of the samples aged for 48 h before acidification and for different aging durations (24, 72 and 120 h) after acidification. A decrease in reflections intensities for the samples with decreased crystallization time after acidification was observed. Thus, it could be concluded that the aging stage after acidification also influences the final crystallinity of hierarchical zeolites.

The degree of microporous structure formation during synthesis of the hierarchical materials can be specified by the thermal analysis. The DTG profiles of the as-synthesized samples are presented in Fig. 3. DTG curve obtained for as-ZSM-5 (Fig. 3a) consists of three regions of weight loss [30-32]. The first region, at temperatures below 100°C, is assigned to desorption of zeolitic water, while the second (100-300°C) and third (>300°C) ones are related to decomposition of structure directing agent (TPAOH) balancing the charge of Si-O<sup>-</sup> groups in the connectivity defects and Al(OSi)<sub>4</sub> within the various types of micropores, respectively. In DTG curve of as-ZSM-5 (24/144) the high temperature peaks connected with TPAOH decomposition occluded within the micropore structure are not present. Additionally, in the DTG profile obtained for this sample a small peak at about 100°C, probably connected with decomposition of organic surfactant present of the surface of amorphous material was detected. These results, which are in agreement with N<sub>2</sub> sorption and XRD analyses, proved that 24 h of hydrothermal crystallization of ZSM-5 synthesis gel before

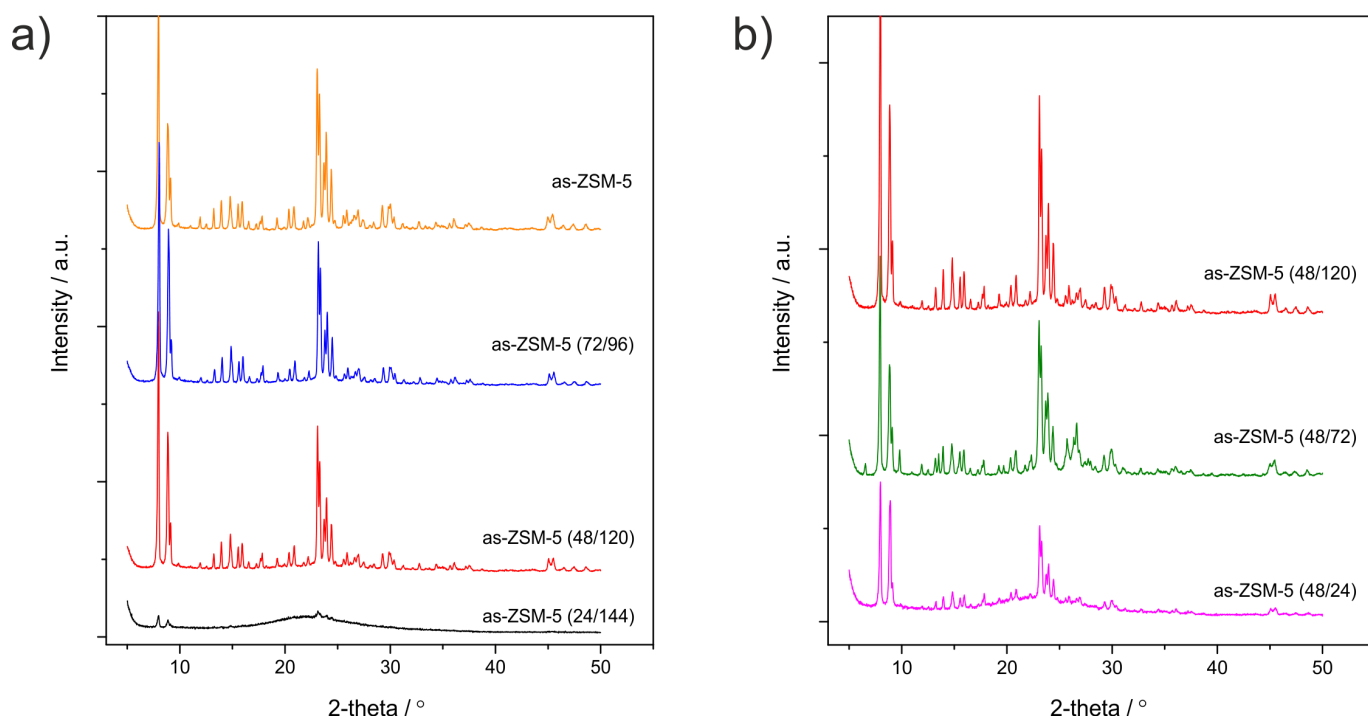


**Fig. 2** XRD patterns of the as-synthesized samples aged for different times before (a) and after (b) acidification

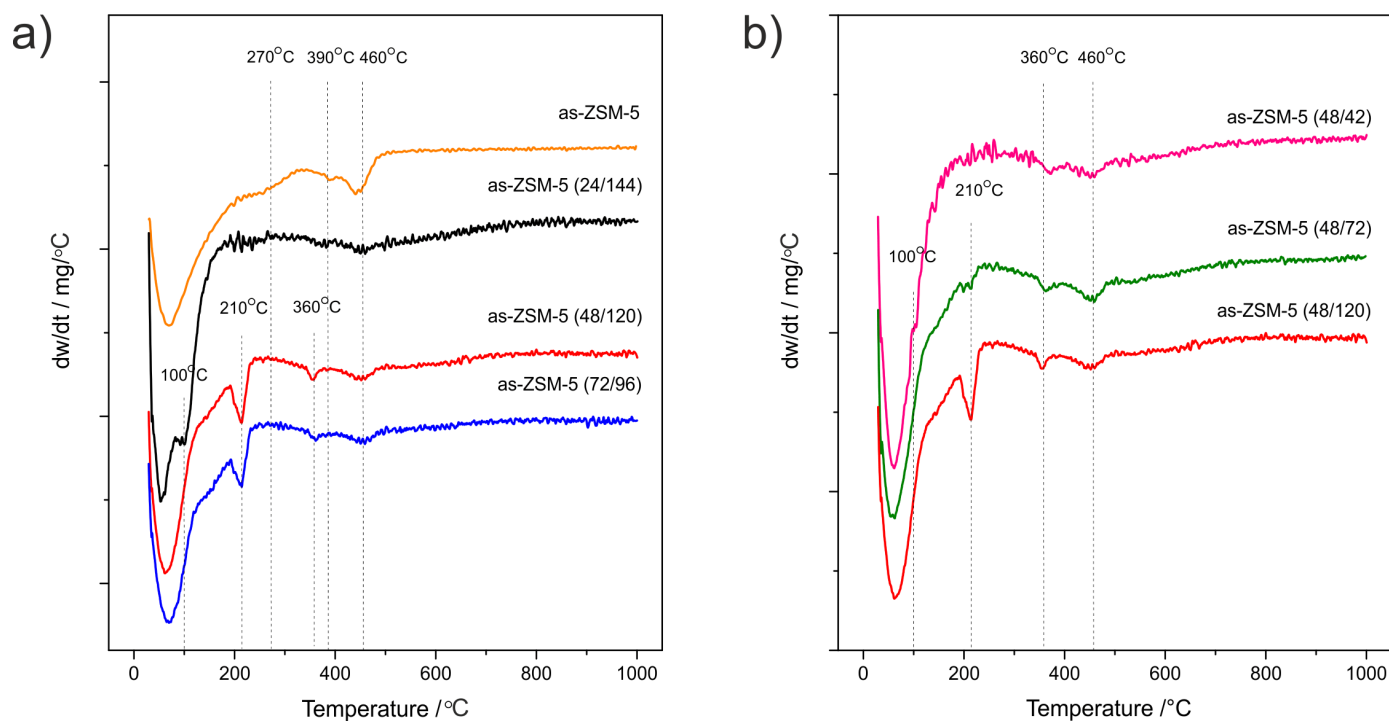


**Fig. 3** DTG profiles of the as-synthesized samples aged for different times before (a) and after (b) acidification

acidification was not enough to form the MFI zeolitic structure. In case of the samples aged for 48 and 72 h (as-ZSM-5 (48/120) and as-ZSM-5(72/96)) weight loss observed in the second region is more intensive than for conventional as-ZSM-5 zeolite. However, the peaks in the third region are less intensive and also shifted to lower temperatures. These changes could be related to shorter crystallization time of the zeolitic phase in case of the micro-mesoporous samples, what results in a weaker incorporation of TPA<sup>+</sup> within the zeolite structure (weaker stabilization in the pore system). In case of the series differing in the aging duration after acidification (Fig. 3b) lower stability of organic surfactants within the micropore structure with decreasing aging duration was observed. An intensive peak at about 210°C, assigned to TPA<sup>+</sup> balancing the connectivity defects in the structure of the micro-mesoporous as-ZSM-5 (48/120) sample, decreased after shortening of the aging duration from 120 to 72 h and disappeared after shortening of this procedure to 24 h. In case of as-ZSM-5 (48/24) this change was connected with an appearance of a small peak at about 100°C (the same as in case of as-ZSM-5 (24/144)), probably related to combustion of TPAOH not interacting with the zeolite matrix.

The Si/Al ratio in the as-synthesized samples was analyzed using the atomic absorption spectroscopy (AAS) method (Tab. 2). The relatively low Si/Al ratio, equal to 12 in case of as-ZSM-5, increased after modification of the porous structure by acidification. Lower Al content in the micro-mesoporous samples can be connected with disturbed and incomplete crystallization of the samples. However, a clear dependency between the duration of zeolites hydrothermal aging and the changes in the Si/Al ratio was not observed. Therefore, it could be concluded that the acidification of the samples with the total duration of hydrothermal aging of 7 days increased the Si/Al ratio to about 20 and the shortening of the aging duration after acidification increased this ratio to about 35. Thus, both these factors acidification and shortening of the crystallization time influenced the Al content in the modified samples.

Temperature-programmed desorption of ammonia (NH<sub>3</sub>-TPD) was used to determine the surface acidity (surface concentration and strength of acid sites) of the as-synthesized samples and their protonic forms (after triple ion-exchange with NH<sub>4</sub>NO<sub>3</sub> followed by calcination). Surface concentration of acid sites (Tab. 3) was calculated by integration of areas under TPD profiles, which were recalculated into a number of adsorbed ammonia molecules (it was assumed that one NH<sub>3</sub> molecule adsorb on one acid site). The total NH<sub>3</sub> uptake obtained in case of as-ZSM-5, equal 819 μmol/g, decreased after modification by acidification of the synthesis gel. This effect could be explained by shorter time of hydrothermal aging and acidification of the hierarchical samples, what disturbed crystallization of the samples and thus resulted in lower amount of framework Al. In case of the samples aged for 48 and 72 h (as-ZSM-5 (48/120) and as-ZSM-5 (72/96)) the concentration of acid sites was equal to 322 and 439, respectively, while in case of as-ZSM-5 (24/144) a significant decrease of this value (26 μmol/g) was observed. Taking into account the similar Si/Al ratio determined for

all three samples by AAS method it could be supposed that substantial part of Al was present in as-ZSM-5 (24/144) in the amorphous and low-surface phase. Shortening of the crystallization time after acidification additionally decreased the concentration of acid sites, what is in agreement with the AAS results.

**Table 3** Concentration of acid sites measured by NH<sub>3</sub> sorption for the as-synthesized samples and their H-forms

Sample code	NH <sub>3</sub> uptake /μmol/g	Sample code	NH <sub>3</sub> uptake /μmol/g
as-ZSM-5	819	H-ZSM-5	925
as-ZSM-5 (24/144)	26	H-ZSM-5 (24)	29
as-ZSM-5 (48/120)	322	H-ZSM-5 (48)	325
as-ZSM-5 (72/96)	439	H-ZSM-5 (72)	420
as-ZSM-5 (48/24)	149	H-ZSM-5 (48/24)	198
as-ZSM-5 (48/72)	190	H-ZSM-5 (48/72)	209

An increase in surface acidity, observed after ion-exchange in case of the majority of the samples, is possibly related to the formation of acid Brønsted sites being structural ≡Al-O(H)-Si≡ groups of the zeolite framework.

NH<sub>3</sub>-TPD profiles of the as-synthesized samples and their H-forms (beside as-ZSM-5 (24/144) and H-ZSM-5 (24/144) with a very low surface density of acid sites) are presented in Figs. 4 a and b, respectively. In the obtained NH<sub>3</sub>-TPD profiles three types of acid sites, with respect to their acidic strength, can be distinguished: (i) at about 200°C attributed to weak acid sites, so called α sites, (ii) at about 300°C attributed to medium acid sites, so called β sites and (iii) at about 400°C attributed to strong acid sites, so called γ sites [33, 34]. The shape of ammonia desorption profile significantly changed after modification of the porous structure by acidification (Fig. 4a). The changes observed after acidification of the zeolite seeds solution can be connected with a partial protonation of the micro-mesoporous samples (using HCl), while in case of the conventional as-ZSM-5 sample directly after synthesis Na-form was obtained.

After ion-exchange to obtain H-forms of the micro-mesoporous samples the shape NH<sub>3</sub> desorption profiles were not changed significantly (only a slight increase in desorption spectra intensity was observed). While, in case of conventional, microporous ZSM-5 the changes were much more significant. After ion-exchange of the samples with NH<sub>4</sub>NO<sub>3</sub> the peak corresponding to β-type acid sites disappeared in favor of high temperature peak at about 400-500°C (γ-type acid sites). The obtained results suggest that by exchange of Na<sup>+</sup> for H<sup>+</sup> the β-type acid sites, which are possibly Lewis type sites were turned into γ-type, which are probably Brønsted acid sites [33].

It is also worth to notice that despite the presence of α- and γ-types acid sites in all the samples of H-form the peaks present in the TPD profile of H-ZSM-5 are shifted to higher temperatures in comparison to the micro-mesoporous samples. It means that the structure disorder caused by the acidification results in acid sites of slightly lower strength in comparison to conventional zeolite.

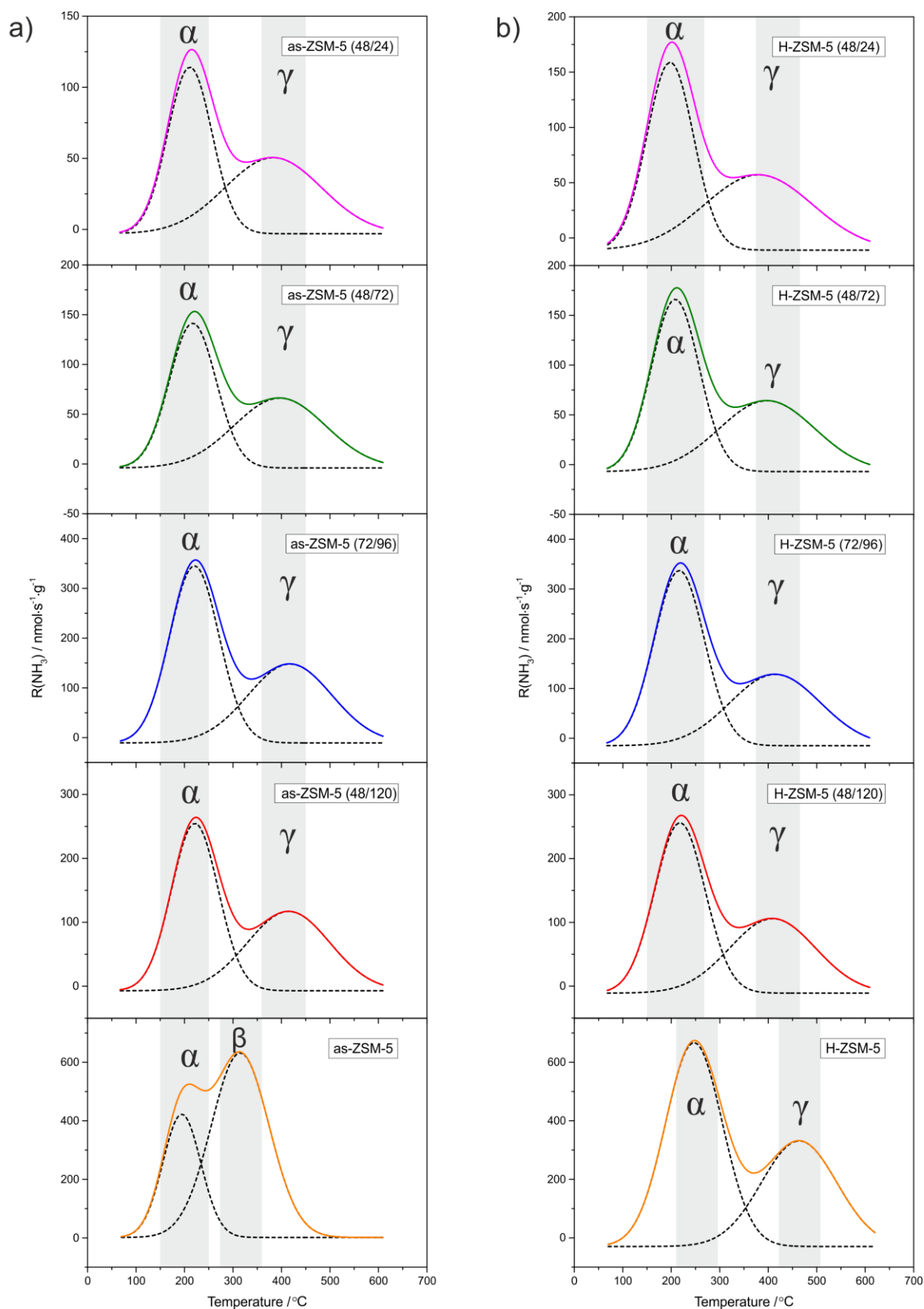


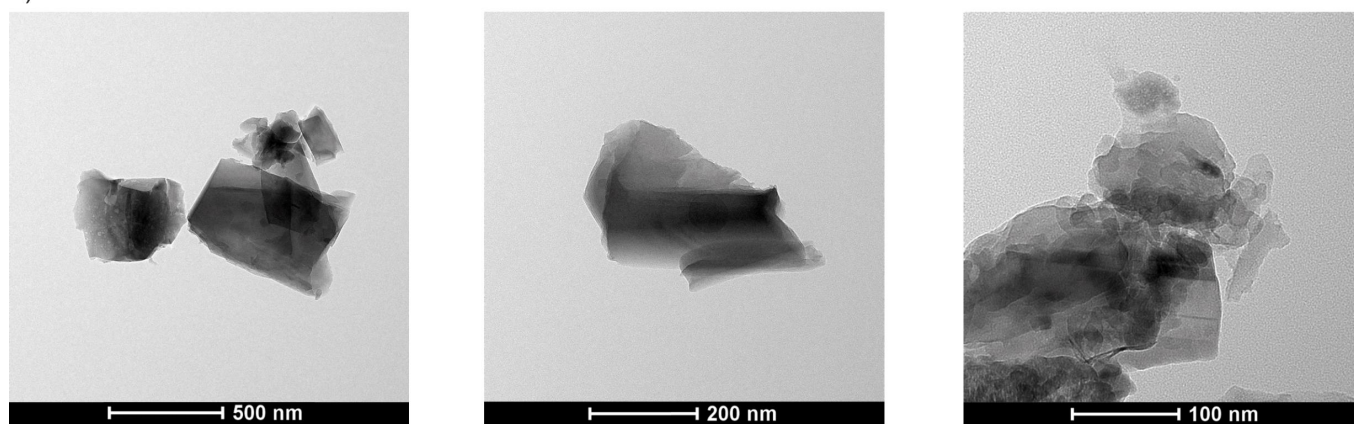
**Fig. 4**  $\text{NH}_3$ -TPD profiles of the as-synthesized samples (a) and their H-forms (b). Conditions: 10000 ppm  $\text{NH}_3$  in He; gas flow 20 ml/min; weight of catalyst - 0.05 g



Bright field transmission electron microscopy (BFTEM) images (Fig. 5) of two selected samples (as-ZSM-5 and as-ZSM-5 (48/120)) give an overview of the conventional and micro-mesoporous materials morphology. The structure of conventional ZSM-5 and the acidified sample differs significantly. In case of the micro-mesoporous sample, zeolite seeds, formed during hydrothermal treatment before acidification, were aggregated (during hydrothermal treatment after acidification) with the formation of the loose, worm-hole like structure. The mesoporosity in the as-ZSM-5 (48/120) sample was generated between the zeolitic seeds of the size of 10-20 nm. Similar morphology of the micro-mesoporous samples was obtained in case of hierarchical Beta zeolite synthesized using the same method (mesotemplate-free method) [12, 14, 15]. In case of both the samples the aluminum distribution determined by EDX analysis was uniform (results not shown).

acidification. The catalytic activity of as-ZSM-5 (48/120) and as-ZSM-5 (72/96) did not differ significantly, what is a result of the similar physicochemical properties of these samples. Maximum methanol conversion in the presence of these samples was obtained at 225°C. Further temperature increase resulted in a slight decrease in methanol conversion, what can be explained by the exothermic character of this reaction [24, 26]. A significant increase in catalytic activity related to the prolongation of aging duration before acidification from 24 to 48 h can be connected with substantial increase in the surface density of acid sites (acid sites are the most likely considered as active centers of the DME synthesis). The changes in methanol conversion observed for the catalysts obtained with increasing duration of hydrothermal treatment was accompanied by a decrease in the reaction selectivity to DME (only at high temperatures). High acidity of the samples is from one side responsible for the catalytic efficiency of

### a) as-ZSM-5



### b) as-ZSM-5 (48/120)

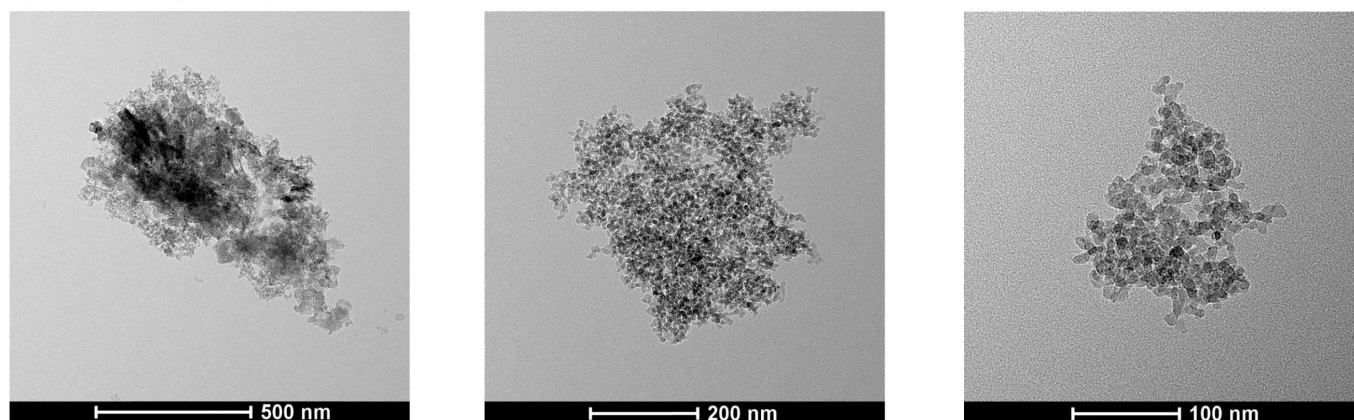


**Fig. 5** BFTEM images of conventional as-ZSM-5 zeolite (a) and the micro-mesoporous as-ZSM-5 (48/120) sample (b) with different magnifications

### 3.2. Catalytic study: MTD Reaction

Results of the catalytic studies of the as-synthesized samples and their H-forms in the process of DME synthesis from methanol are presented in Figs. 6 and 7, respectively. The methanol conversion over the as-synthesized micro-mesoporous samples (Fig. 6a) increased with the increasing of the aging duration before

methanol conversion, however, on the other side is a cause of byproducts formation. The sample as-ZSM-5, despite the highest concentration of acid sites among the examined samples, was completely inactive in methanol conversion. This result suggests that not only concentration of acid sites, but also their strength ( $\text{NH}_3$ -TPD profile of this sample significantly

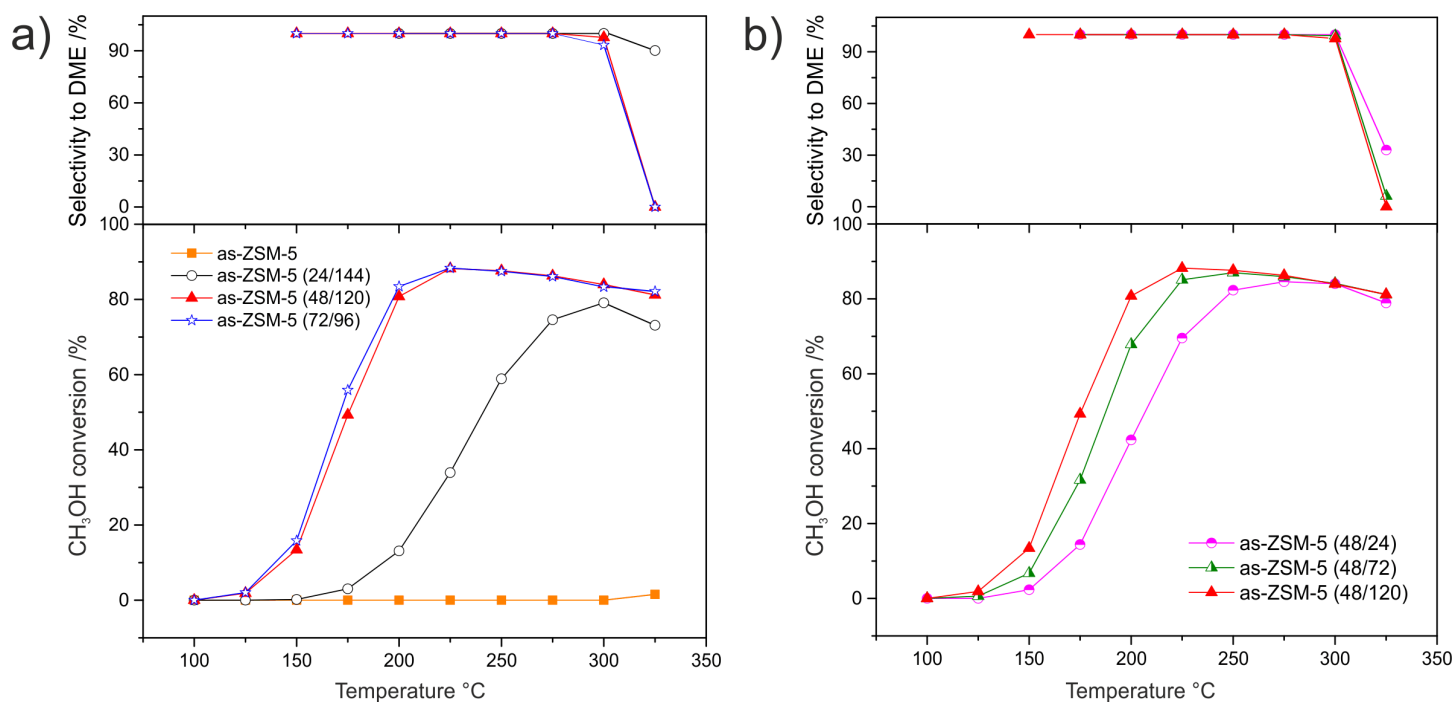


**Fig. 6** Temperature dependence of CH<sub>3</sub>OH conversion and selectivity to DME over the as-synthesized samples aged for different times before (a) and after (b) acidification. Conditions: 4 vol. % CH<sub>3</sub>OH; He as balancing gas; total flow rate - 20 ml/min; weight of catalyst - 0.1 g

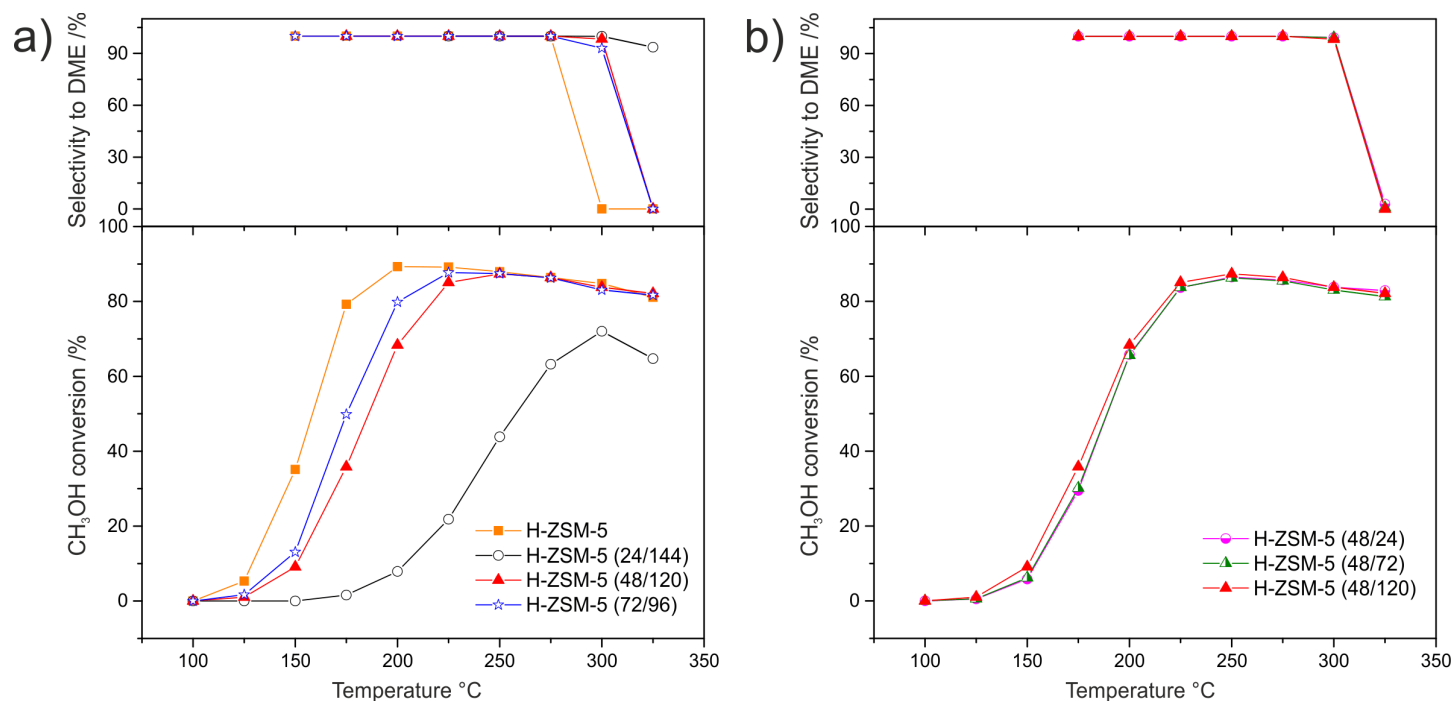


**Fig. 7** Temperature dependence of CH<sub>3</sub>OH conversion and selectivity to DME over H-forms of the samples aged for different times before (a) and after (b) acidification. Conditions: 4 vol. % CH<sub>3</sub>OH; He as balancing gas; total flow rate - 20 ml/min; weight of catalyst - 0.1 g

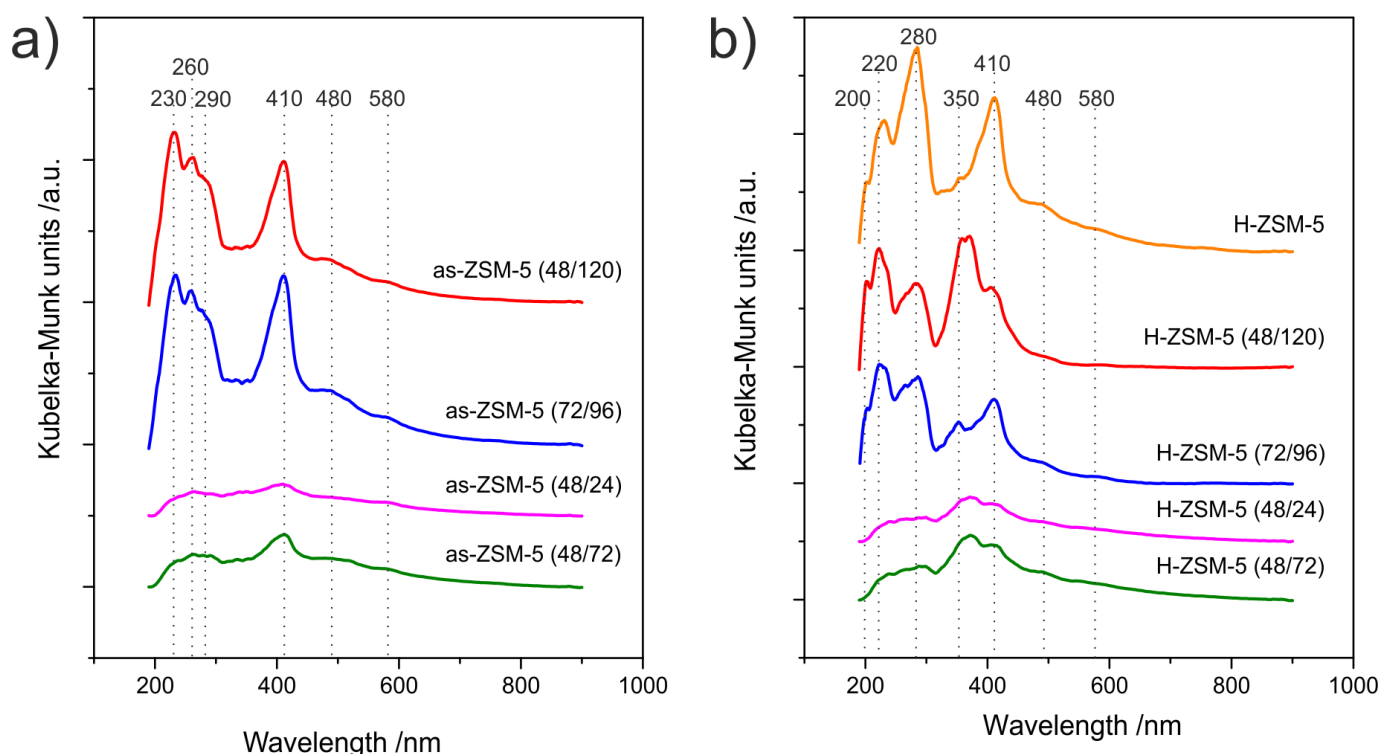
differ from those obtained for other samples of this series) is essential in DME synthesis from methanol. The shortening of the aging duration after acidification (Fig. 6b) slightly decreased the methanol conversion and increased the selectivity to DME. This effect can be associated with a decrease in the surface density of acid sites observed for the samples with shortened hydrothermal treatment after acidification.

The most significant changes in the catalytic activity of the samples after ion-exchange to H-form were observed in case of the H-ZSM-5 sample (Fig. 7a). The as-ZSM-5 catalyst, which was completely inactive, after ion-exchange to H-form showed the highest methanol conversion among the examined samples. Thus, it could be concluded that the strong acid sites, of  $\gamma$ -type are responsible for methanol dehydration to DME. On the other side, the presence of strong acid sites in H-ZSM-5 decreased the reaction selectivity to DME. Dimethyl ether was not detected in the outlet gases at temperature about 25°C lower in comparison to the reaction performed in the presence of the hierarchical samples.

In case of the samples aged for different times after acidification (Fig. 7b) the ion-exchange to H-forms resulted in a very similar activity in methanol conversion and selectivity to DME for all three samples (H-ZSM-5 (48/120), H-ZSM-5 (48/24) and H-ZSM-5 (48/72)). It was connected with the increased acidity of H-ZSM-5 (48/24) and H-ZSM-5 (48/72) after ion-exchange with  $\text{NH}_4\text{NO}_3$ . Thus, it could be concluded that the change in duration of hydrothermal treatment after acidification did not influence the catalytic activity of the samples in the process of DME synthesis.

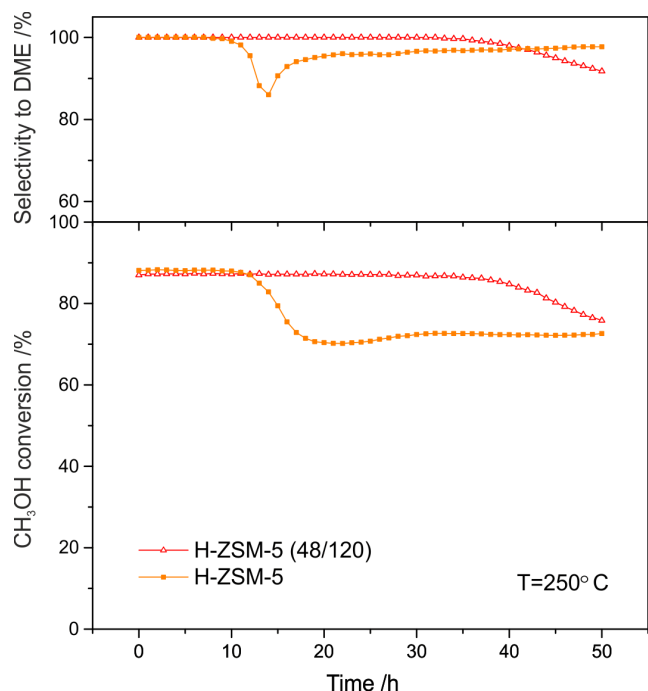
It should be also stressed that the relatively high activity of the hierarchical samples was obtained directly after synthesis (as-form of the samples), while in case of as-ZSM-5 an additional synthesis step was needed for activation of this sample in the considered catalytic reaction.

Methanol conversion resulted not only in the formation of desired DME but also side products (polyolefins, aromatic compounds and carbon deposits) responsible for gradual deactivation of the catalysts by blocking of active sites. Moreover, during aging of such deposits (growth of polycyclic aromatic structures) the zeolite pore system can be blocked, what decreases the efficiency of internal diffusion of reactants [35]. The chemical nature of the formed coke deposit was analyzed using UV-vis-DRS technique. Figs. 8a and b show the UV-vis-DR spectra obtained for the as-synthesized samples and their H-forms after catalytic test (only for the samples in which case coke deposit was formed) of methanol conversion, respectively. In case of the as-synthesized samples (Fig. 8a) six absorption bands with different intensity were identified. The bands in a first region (200-300 nm) may be ascribed to dienes, cyclohexadiene, benzene or substituted benzenes. While, the bands in a second region (400-600 nm) can be attributed to bulky aromatic species, like diphenyl, polyphenyl carbenium ions, polyalkylaromatics or condensated aromatic ring system [36, 37]. The intensity of these bands increased together with an increase of the samples acidity. Conversion of zeolites to their H-forms by ion-exchange resulted in the formation of new bands in the UV-vis-DR



**Fig. 8** UV-vis difference spectra of carbon deposit formed during catalytic reaction of the as-synthesized samples (a) and their H-forms (b)

spectra, what proves more complex structure of carbon deposits (greater heterogeneity of coke species). It is probably related to the enhanced Brønsted acidity of the samples.



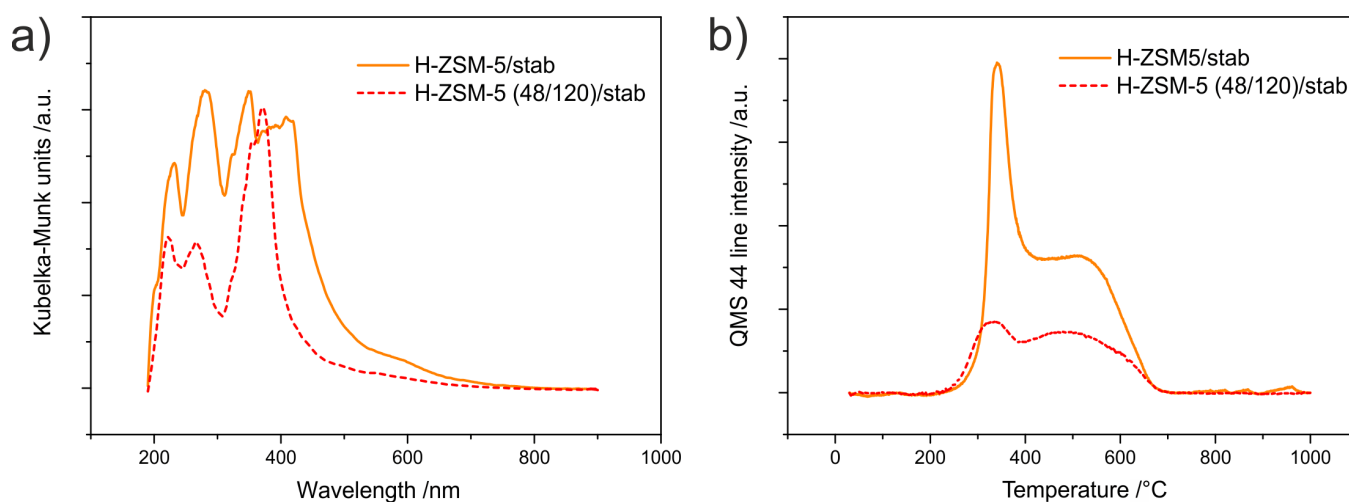
**Fig. 9** Time dependence (stability tests: 50 h at 250°C) of CH<sub>3</sub>OH conversion and selectivity to DME of H-ZSM-5 and H-ZSM-5 (48/120). Conditions: 4 vol. % CH<sub>3</sub>OH; He as balancing gas; total flow rate - 20 ml/min; weight of catalyst - 0.1 g

Fig. 9 shows the results of stability tests (50 h of continuous work at 250°C) for two selected catalysts - parent H-ZSM-5 and micro-mesoporous H-ZSM-5 (48/120) (temperature of the stability tests was adjusted to analyze the catalysts stability for methanol conversion of about 90%). The methanol conversion in the presence

of parent H-ZSM-5 decreased by about 20% after 18 h of time on stream and subsequently stabilized at about 70%. In case of the hierarchical sample the methanol conversion remained at constant level for a longer time on stream than in case of conventional zeolite.

After 35 h of continuous work the methanol conversion started progressively drop to about 75% (after 50 h of test). The changes in catalyst activity were accompanied by the changes in reaction selectivity to DME. In case of H-ZSM-5 a sharp decline in selectivity to DME after 10 h of stability test, which subsequently progressively increased to about 97%, was observed. In case of H-ZSM-5 (48/120) selectivity to DME started to decrease after 35 h of time on stream, what was continued to about 92% after 50 h of the stability test. It could be concluded that during first 35 h hours of stability test better results were obtained for the hierarchical sample. However, at the end of the stability test, both the conversion and selectivity to DME obtained over H-ZSM-5 seem to stabilize, while in case of H-ZSM-5 (48/120) both values were progressively dropping. Possibly during first hours of the catalytic test the micro-mesoporous structure is more resistant for the side-products formation and deactivation by coke deposits. Although, after larger times on stream both structures (microporous and hierarchical) behave similar.

The chemical nature of carbon deposits formed during stability test (samples marked as H-ZSM-5/stab and H-ZSM-5 (48/120)/stab) was analyzed by two experimental methods - UV-vis-DR spectroscopy and thermogravimetric analysis coupled with QMS detection of gas products (Figs. 10a and b respectively). In case of H-ZSM-5/stab (Fig. 10a) the spectrum contains more bands than the spectrum of the hierarchical sample (H-ZSM-5 (48/120)/stab), what is an evidence of the higher heterogeneity of the coke deposits. Moreover, the intensity of the bands in spectrum of conventional zeolite is greater in comparison to the micro-mesoporous sample, especially at higher wavelengths. It proves the presence of polycondensed aromatics of higher condensation.



**Fig. 10** UV-vis difference spectra of carbon deposit (a) and CO<sub>2</sub> evolution signals measured by QMS of the samples after stability test

Only one band in the spectra of H-ZSM-5 (48/120)/stab, located at about 370 nm and attributed to conjugated double bonds and polycondensed aromatics [37], is characterized by higher intensity.

In case of both the samples, an evolution of CO<sub>2</sub> (Fig. 10b) at relatively low temperature as well as the evolution in the same temperature range of water vapour (m/e=18) (results not shown) suggests that formed coke deposits apart from carbon contain also hydrogen. For the H-ZSM-5/stab sample the evolution of higher amount of CO<sub>2</sub> was detected. The weight loss connected with carbon deposits burning measured in case of this sample was equal to about 6.5%, while in case of the hierarchical sample to 2.5%. For both the samples two peaks of CO<sub>2</sub> evolution were identified. These peaks can be related to different nature of formed coke. The first peak, at about 340°C, can be attributed to slightly developed coke, while the second one, at about 510°C, to its more condensed forms (with a lower H/C ratio) [38].

## Conclusions

In the frame of undertaken studies a new synthesis method of micro-mesoporous materials with ZSM-5 properties was developed. The obtained samples were studied in the role of the catalysts for synthesis of DME from methanol. The catalytic performance of the zeolitic samples was correlated with their properties - porosity, acidity and crystallinity.

Two parameters - duration of the hydrothermal treatment (i) before and (ii) after acidification were selected as parameters for the synthesis optimization leading to the effective catalysts for DME production.

The most important results of the studies can be summarized as follows:

- Nano-seeds of ZSM-5 zeolite are being created during first 48 h of hydrothermal treatment of the synthesis mixture (it was shown that 24 h of the sample aging was not enough to generate the zeolite properties in the final material).
- 48 h of hydrothermal treatment followed by acidification and secondary aging period resulted in micro-mesoporous material with partially preserved properties of MFI topology (crystallinity, acidity). Further prolongation of this time did not change significantly the final properties of the hierarchical material, thus 48 h was chosen as optimal aging time before acidification.
- The shortening of the crystallization time after acidification resulted in a decrease of the textural parameters, acidity and crystallinity of the samples. It means that both stages of hydrothermal treatment have a strong impact on the final properties of the samples and the optimum properties were obtained for the sample as-ZSM-5 (48/120) (48 h of aging before acidification, followed by 120 h of aging after acidification).
- The as-ZSM-5 (48/120) and as-ZSM-5 (72/96) samples showed the highest activity in the process of dimethyl ether synthesis among the obtained hierarchical samples (88% of methanol conversion at 225°C).
- The as-ZSM-5 sample (Na-form) was inactive in methanol conversion, while after ion-exchange to H-form showed very

high activity. The high catalytic efficiency in this reaction was connected with the presence of strong acid sites of  $\gamma$ -type (acid sites of Brønsted type) present in the samples after ion-exchange to H-form.

- The as-synthesized micro-mesoporous samples showed high catalytic activity, while in case of conventional zeolite an additional synthesis step, ion exchange to obtain its H-form, was necessary to induce the catalytic activity.
- Lower concentration of surface acid sites in case of the micro-mesoporous samples (as-ZSM-5 (48/120) and as-ZSM-5 (72/96)) was a cause of slight decrease in methanol conversion in comparison to conventional zeolite. However, on the other side, the presence of weaker acid sites connected with generated mesoporosity resulted in the improved reaction selectivity to DME.
- Results of the stability test (50 h on stream) performed for H-ZSM-5 and H-ZSM-5 (48/120) as well as the analysis of the spent catalysts, showed that the sample with the hierarchical porous structure was more stable (especially during first hours of the stability test) and more resistant for the carbon deposits formation.

## Acknowledgements

This work was supported by the National Science Center under grant no. 2011/03/N/ST5/04820. Part of the research was carried out with the equipment purchased thanks to the financial support of the European Regional Development Fund in the framework of the Polish Innovation Economy Operational Program (contract no. POIG.02.01.00-12-023/08). U.D. thanks to Spanish Government by the funding (project MAT2014-52085-C2-1-P).

## Notes and references

- [1] D. Verboekend, J. Pérez-Ramírez, *Catal. Sci. Technol.*, 2011, **1**, 879
- [2] D. Verboekend, J. Pérez-Ramírez, *Chem. Eur. J.*, 2011, **17**, 1137
- [3] L. Jin, H. Hu, S. Zhu, B. Ma, *Catal. Today*, 2010, **149**, 207
- [4] L.H. Ong, M. Dömök, R. Olindo, A.C. van Veen, J.A. Lercher, *Micropor. Mesopor. Mater.*, 2012, **164**, 9
- [5] J-B. Koo, N. Jiang, S. Saravanamurugan, M. Bejblová, Z. Musilová, J. Čejka, S-E. Park, *J. Catal.*, 2010, **276**, 327
- [6] L. Wang, Z. Zhang, C. Yin, Z. Shan, F-S. Xiao, *Micropor. Mesopor. Mat.*, 2010, **131**, 58
- [7] Y. Zhu, Z. Hua, J. Zhou, L. Wang, J. Zhao, Y. Gong, W. Wu, M. Ruan, J. Shi, *Chem. Eur. J.*, 2011, **17**, 14618
- [8] M. Choi, K. Na, J. Kim, Y. Sakamoto, O. Terasaki, R. Ryoo, *Nature*, 2009, **461**, 246
- [9] K. Na, M. Choi, W. Park, Y. Sakamoto, O. Terasaki, R. Ryoo, *J. Am. Chem. Soc.*, 2010, **132**, 4169
- [10] X. Zhang, D. Liu, D. Xu, S. Asahina, K.A. Cychosz, K. Varoon Agrawal, Y. Al Wahedi, A. Bhan, S. Al Hashimi, O. Terasaki, M. Thommes, M. Tsapatsis, *Science*, 2012, **336**, 1684
- [11] L. Tosheva, V.P. Valtchev, *Chem. Mater.*, 2005, **17(10)**, 2494
- [12] M. Rutkowska, L. Chmielarz, D. Macina, Z. Piwowarska, B. Dudek, A. Adamski, S. Witkowski, Z. Sojka, L. Obalová, C.J. Van Oers, P. Cool, *Appl. Catal. B: Environ.*, 2014, **146**, 112
- [13] M. Rutkowska, Z. Piwowarska, E. Micek, L. Chmielarz, *Micropor. Mesopor. Mater.*, 2015, 209, 54

- [14] C.J. Van Oers, W.J.J. Stevens, E. Bruijn, M. Mertens, O.I. Lebedev, G. Van Tendeloo, V. Meynen, P. Cool, *Micropor. Mesopor. Mater.*, 2009, **120**, 29
- [15] C.J. Van Oers, M. Kurttepel, M. Mertens, S. Bals, V. Meynen, P. Cool, *Micropor. Mesopor. Mater.*, 2014, **185**, 204
- [16] J. Sun, G. Yang, Y. Yoneyama, N. Tsubaki, *ACS Catal.*, 2014, **4**, 3346
- [17] Z. Azizi, M. Rezaeimanesh, T. Tohidian, M. R. Rahimpour, *Chem. Eng. Proc.*, 2014, **82**, 150
- [18] S. Hassanpour, M. Taghizadeh, *Ind. Eng. Chem. Res.*, 2010, **49**, 4063
- [19] A.A. Rownaghi, F. Rezaei, M. Stante, J. Hedlund, *Appl. Catal. B: Environ.*, 2012, **119-120**, 56
- [20] G. Laugel, X. Nitsch, F. Ocampo, B. Louis, *Appl. Catal. A: Gen.*, 2011, **402**, 139
- [21] M. Rutkowska, D. Macina, N. Mirocha-Kubieñ, Z. Piwowarska, L. Chmielarz, *Appl. Catal. B: Environ.*, 2015, **174**, 336
- [22] Y. Wei, P.E. de Jongh, M.L.M. Bonati, D.J. Law, G.J. Sunley, K.P. de Jong, *Appl. Catal. A: Gen.*, 2015, **504**, 211
- [23] Q. Yang, H. Zhang, M. Kong, X. Bao, J. Fei, X. Zheng, *Chinese J. Catal.*, 2013, **34**, 1576
- [24] H. Li, S. He, K. Ma, Q. Wu, Q. Jiao, K. Sun, *Appl. Catal. A: Gen.*, 2013, **450**, 152
- [25] Y. Sang, H. Liu, S. He, H. Li, Q. Jiao, Q. Wu, K. Sun, *J. Energ. Chem.*, 2013, **22**, 769
- [26] Q. Tang, H. Xu, Y. Zheng, J. Wang, H. Li, J. Zhang, *Appl. Catal. A: Gen.*, 2012, **413-414**, 36
- [27] H. Robson, K.P. Lillerud, *Verified Synthesis of Zeolitic Materials*, Elsevier, 2001, ISBN: 0-444-50703-5
- [28] J. Rouquerol, P. Llewellyn, F. Rouquerol, *Stud. Surf. Sci. Catal.*, 2007, **160**, 49
- [29] M. Thommes, K. Kaneko, A.V. Neimark, J.P. Olivier, F. Rodriguez-Reinoso, J. Rouquerol, K.S.W. Sing, *Pure Appl. Chem.*, 2015, **87(9-10)**, 1051
- [30] T. Xue, Y.M. Wang, M-Y. He, *Micropor. Mesopor. Mater.*, 2012, **156**, 29
- [31] M. Singh, R. Kamble, N. Viswanadham, *Catal. Lett.*, 2008, **120**, 288
- [32] M.M. Mohamed, F.I. Zidan, M.H. Fodail, *J. Mater. Sci.*, 2007, **42**, 4066
- [33] J-H. Kim, M.J. Park, S.J. Kim, O-S. Joo, K-D. Jung, *Appl. Catal. A: Gen.*, 2004, **264**, 37
- [34] G. Bonura, M. Cordaro, L. Spadaro, C. Cannilla, F. Arena, F. Frusteri, *Appl. Catal. B: Environ.*, 2013, **140-141**, 16
- [35] D. Mores, J. Kornatowski, U. Olsbye, B.M. Weckhuysen, *Chem. Eur. J.*, 2011, **17**, 2874
- [36] H.G. Karge, *Stud. Surf. Sci. Catal.*, 2001, **137**, 707
- [37] P. Castaño, G. Elordi, M. Olazar, A.T. Aguayo, B. Pawelec, J. Bilbao, *Appl. Catal. B: Environ.*, 2011, **104**, 91
- [38] G. Elordi, M. Olazar, G. Lopez, P. Castaño, J. Bilbao, *Appl. Catal. B: Environ.*, 2011, **102**, 224